Determination of Bolt Forces and Normal Contact Pressure Between Elements in the System With Many Bolts for its Assembly Conditions

Rafał Grzejda[1]

[1] Faculty of Mechanical Engineering and Mechatronics, West Pomeranian University of Technology, Szczecin, 19 Piastow Ave., 70-310 Szczecin, Poland, e-mail: rafal.grzejda@zut.edu.pl

ABSTRACT

The paper put forward a thesis that modelling dissymmetric non-linear multi-bolted connections as a system is possible. Modelling of the systems composed of four subsystems on the assembly state was presented. These subsystems included: a couple of joined elements (a flange and a support), a contact layer between them, and bolts. The physical model of the system was described considering the tightening of bolts according to a specific sequence. In this model: the flange and the support were built using spatial finite elements, the contact layer was formed as the non-linear Winkler model, and the bolts were replaced with simplified models made of flexible beams. The calculation model which can be applied to determine the changes in bolt forces, as well as in the normal contact pressure between the joined elements during the tightening of the system and at its end, was presented. The results of sample calculations for the selected multi-bolted system were shown.

Keywords: multi-bolted system, non-linearity, FE-modelling, Winkler contact model, preload

INTRODUCTION

Multi-bolted connections are frequently applied in mechanical and civil engineering. Most often, they can occur in two states of loading and deformation. The first one is the assembly state in which the connection may be set up under different assembly patterns [2, 32]. Another feature of multi-bolted connections is that they are constructed of many structural components [7, 22, 27, 28]. Due to irregular geometrical structures on the contact surfaces of the joined elements, these connections are usually treated as non-linear [33]. The subject of this paper is modelling of multi-bolted connections regarded as a non-linear system for the assembly condition.

The papers on modelling and calculations of bolted connections relate either to simple single-bolted joints [10, 29] or typical multi-bolted joints [3, 4, 6, 8, 15, 17, 20, 23, 24]. Esmaeili, Zehsaz, Chakherlou and Hasanifard [10] investigated the impact of the clamping force on the fatigue life of double lap bolted connections, while Sadigh and Marami [29] studied the failure behaviour of single lap bolted connections. The modelling of multi-bolted lap connections was discussed in the papers of Ascione [3], Chowdhury, Chiu, Wang and Chang [8], and Kędra and Rucka [17]. Brunesi, Nascimbene and Rassati [4], Chen and Shi [6], and Moradi and Alam [23] published the results of their research on multi-bolted beam-to-column connections. In contrast, Jakubowski and Schmidt [15], Liu, He, Wang, Yang, Pu and Ailin [20], and Mourya, Banerjee and Sreedhar [24] described results of modelling and calculations of multi-bolted flange connections.

In all the afore-mentioned publications, a systemic approach to modelling, calculation and analysing multi-bolted connections was not undertaken.

The most popular method of modelling multi-bolted connections is the finite element method (FEM). While the joined elements in such connections are created mainly as a spatial body, the bolts are modelled in different ways. In addition

to the spatial models of bolts [1, 6, 32], the following substitute FE-models of bolts are used:
- no-bolt models [5],
- spring models [19, 21],
- truss models [9, 30],
- beam models [11, 16, 31],
- rigid body bolt models [14, 25, 26],
- spider bolt models [18].

The FEM was also used in this paper for modelling and calculations of the multi-bolted system. The presented paper constitutes a continuation of the previous publication on modelling non-linear multi-bolted systems [14] in which the distribution of preload in bolts were analysed in the system model with the rigid body bolt models. The current paper concerns the analysis pertaining to preload of bolts distributions and distributions of normal contact pressure between the joined elements in the system model with the spider bolt models.

MODEL OF THE MULTI-BOLTED SYSTEM

The concept of system approach to modelling multi-bolted connections was presented earlier at the 3rd Polish Congress of Mechanics [13].

The model was built from the four subsystems (Fig. 1):
- B – i-element set of the bolts (for i = 1, 2, 3, …, k),
- F – flexible flange element,
- C – j-element contact layer (for j = 1, 2, 3, …, l),
- S – flexible support.

The spider bolt model was used as a single bolt model in the system; the plain part of the bolt and its head were modelled with use of beam elements but the total volume of the beam elements for the head was assumed to be equal to the volume of the head of the real bolt.

Generation of the contact layer model begins with the division of the contact surface between the flange and the support into elementary contact areas. Then, the following are added to the model:
- mesh nodes in the centres of gravity of the elementary contact areas,
- non-linear springs at the nodes identified in the previous step,
- 2D finite element mesh on the contact surface considering the position of the non-linear springs.

The presented method enables the modelling of the contact layer with the characteristics obtained experimentally separately for each element of this layer.
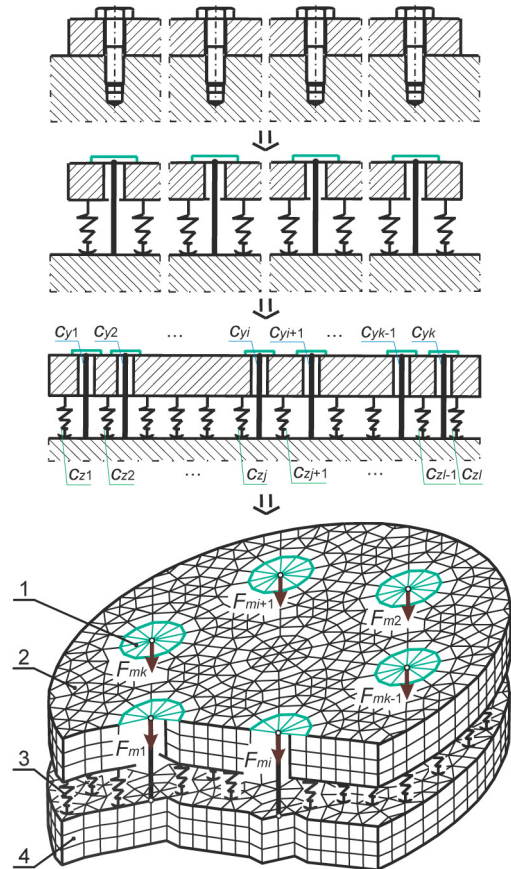

Fig. 1. Multi-bolted system with the spider bolt models (1 – subsystem B, the bolts; 2 – subsystem F, the flexible flange element; 3 – subsystem C, the contact layer; 4 – subsystem S, the flexible support).

On the basis of the 2D finite element mesh on the contact surface between the flange and the support, a uniform 3D finite element mesh was created for the entire volume of the joined elements.

After taking into consideration the division of the multi-bolted system into subsystems, the equation of system equilibrium can be presented in the form [13]:

$$\begin{bmatrix} \boldsymbol{K}_{BB} & \boldsymbol{K}_{BF} & \boldsymbol{0} & \boldsymbol{K}_{BS} \\ \boldsymbol{K}_{FB} & \boldsymbol{K}_{FF} & \boldsymbol{K}_{FC} & \boldsymbol{0} \\ \boldsymbol{0} & \boldsymbol{K}_{CF} & \boldsymbol{K}_{CC} & \boldsymbol{K}_{CS} \\ \boldsymbol{K}_{SB} & \boldsymbol{0} & \boldsymbol{K}_{SC} & \boldsymbol{K}_{SS} \end{bmatrix} \cdot \begin{bmatrix} \boldsymbol{q}_B \\ \boldsymbol{q}_F \\ \boldsymbol{q}_C \\ \boldsymbol{q}_S \end{bmatrix} = \begin{bmatrix} \boldsymbol{p}_B \\ \boldsymbol{p}_F \\ \boldsymbol{p}_C \\ \boldsymbol{p}_S \end{bmatrix} \quad (1)$$

where: $\boldsymbol{K}_{XX}$ denotes the stiffness matrix of the X-th subsystem, $\boldsymbol{K}_{XY}$ is the matrix of elastic couplings between X-th and Y-th subsystems, $\boldsymbol{q}_X$ is the vector of displacements of the X-th subsystem, and $\boldsymbol{p}_X$ denotes the vector of loads of the X-th subsystem, (X and Y are the symbols of the subsystems, $X = Y = \{B, F, C, S\}$).

CALCULATIONS OF THE MULTI-BOLTED SYSTEM ON THE ASSEMBLY STATE

Sample calculations were performed for a selected asymmetrical multi-bolted system shown in Figure 2a.

The model was built using the Midas NFX 2017 program. The connection is fastened using seven M10 bolts made in the class of mechanical properties 8.8. The physical properties of the alloy steel used in the connection model for the bolts and the joined elements are shown in Table 1.

Calculations were performed for the joined elements with a thickness of 20 mm. The outer contours of the flange element and the support can be placed inside a rectangle with sides 110 mm and 125 mm.

The model of the system was fastened in the manner shown in Figure 2a by receiving:

Table 1. Material properties of the steel used for the bolts and the joined elements in the connection model

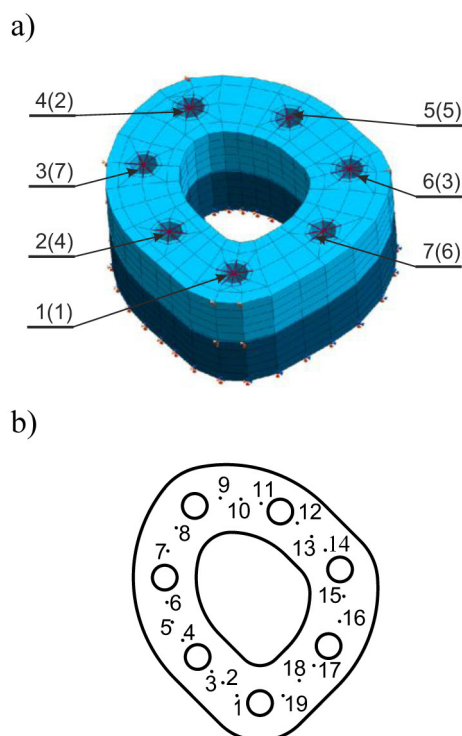| Young's modulus (GPa)	210
Poisson's ratio	0.28

a)

b)

Fig. 2. Analysed multi-bolted system: a) FEM-based model with the numbering of the bolts and the tightening sequence given in parentheses, b) nodes on the contact surface of the joined elements adopted to describe normal contact pressure distributions.

- all degrees of freedom on the bottom surface of the support,
- degrees of freedom in a plane perpendicular to the axis of the bolts in five nodes lying on the outline of the upper surfaces of the flange and the support.

The preload of bolts was set at 20 kN. The tightening sequence is given in parentheses in Figure 2a.

Between the joined elements, a Winkler type of the contact layer built from a set of non-linear springs was introduced. The stiffness characteristics of the springs are described by the following experimentally determined function [12]:

$$R_j = A_j \cdot \left(3.428 \cdot u_j^{1.657}\right) \qquad (2)$$

where: R_j denotes the force in the centre of the j-th elementary contact area, A_j is the j-th elementary contact area, and u_j denotes the deformation of the j-th non-linear spring of the contact layer.

As a result of the calculations, preload of bolts distributions and distributions of normal contact pressure between the joined elements during the tightening process and at the end of this process were obtained.

In Figure 3 variations of the preload in individual bolts during the tightening process of the multi-bolted system are shown as follows:

- in the first line – the preload distribution in bolts No. 1 and No. 4, which were tightened as the first and as the second bolt, respectively,
- in the second line – the preload distribution in bolts No. 6 and No. 2, which were tightened as the third and the fourth bolt, respectively,
- in the third line – the preload distribution in bolts No. 5, No. 7 and No. 3, which were tightened as the fifth, the sixth and the seventh bolt, respectively.

In contrast, the diagrams of normal contact pressure on elementary surfaces on the line joining the nodes defined in Figure 2b during the tightening process of the multi-bolted system are shown in Figure 4.

As the last graph, the scatter of the final preload distribution in the bolts at the end of the tightening process is presented in Figure 5.

On the basis of the obtained results it can be seen that the distributions of the preload of the bolts as well as normal contact pressure between
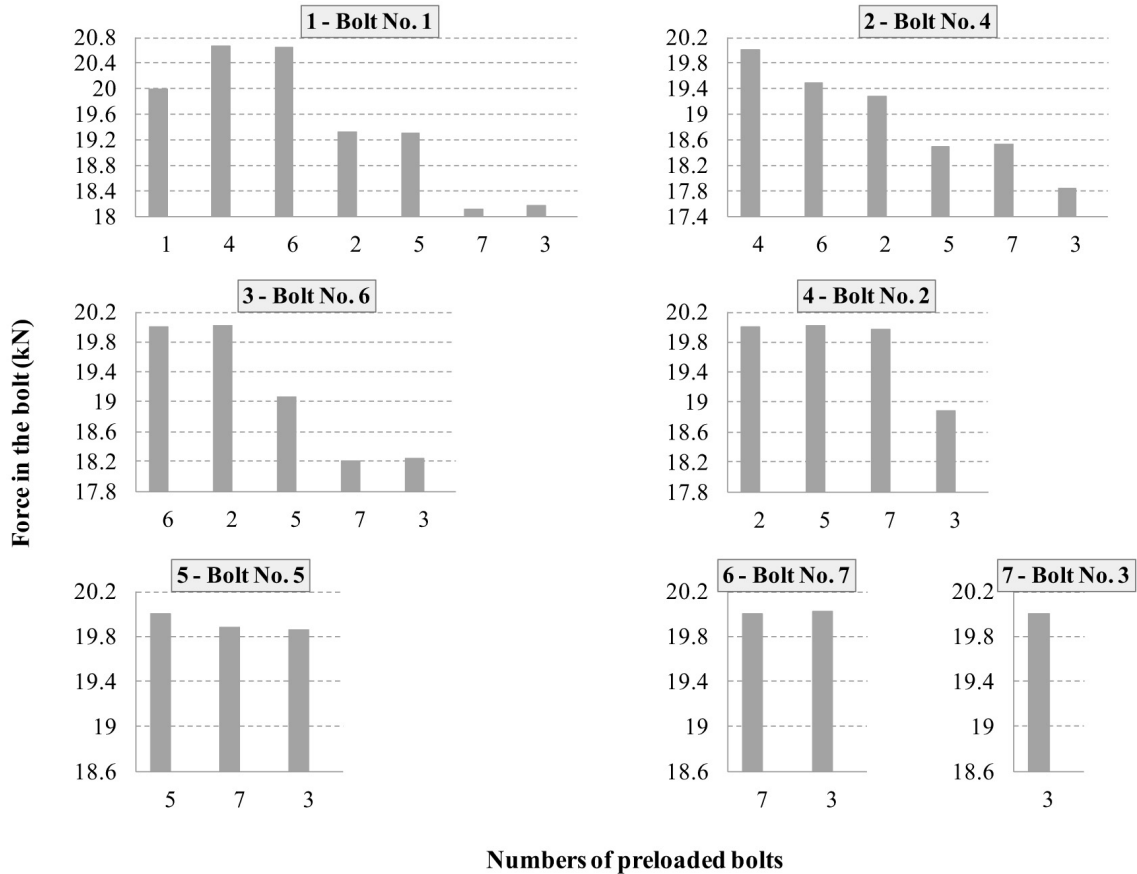
Fig. 3. Preload distributions in the bolts during the tightening process of the multi-bolted system.
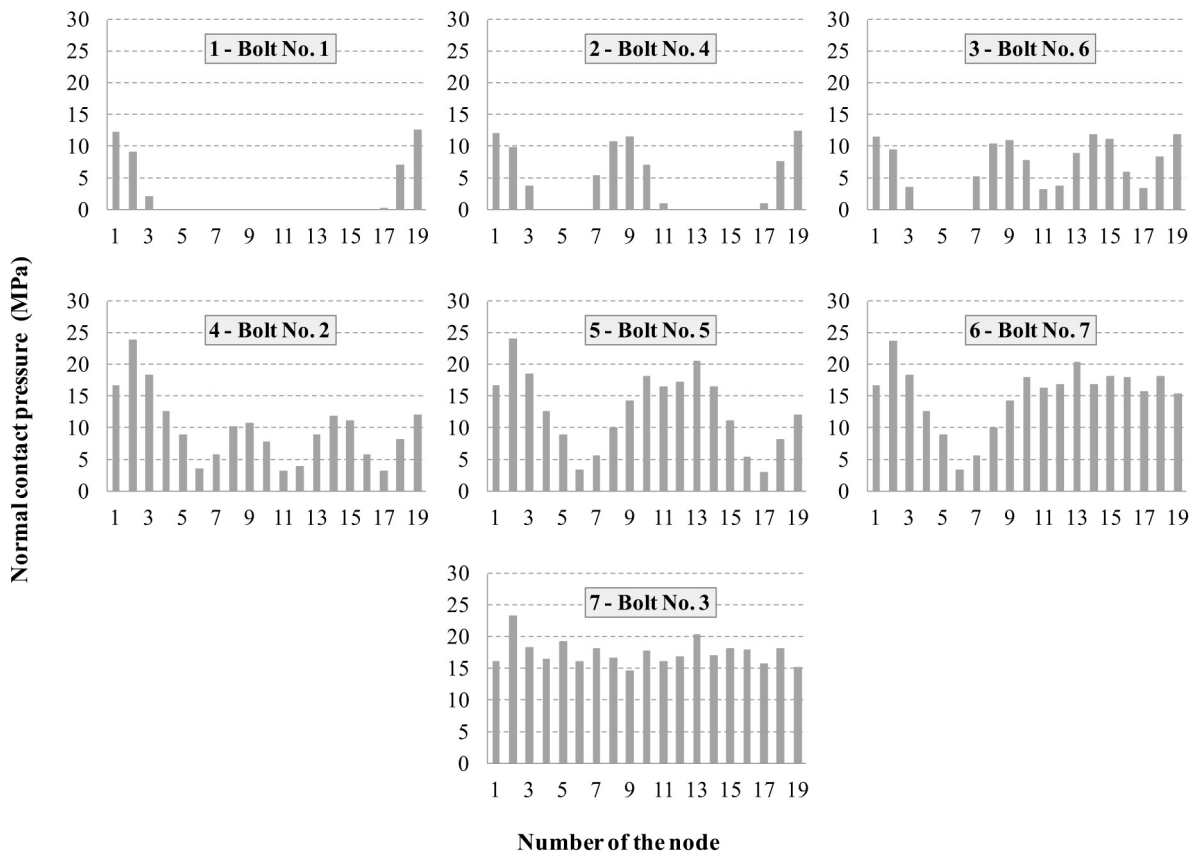

Fig. 4. Diagrams of normal contact pressure on the contact surface of the joined elements during the tightening process of the multi-bolted system.
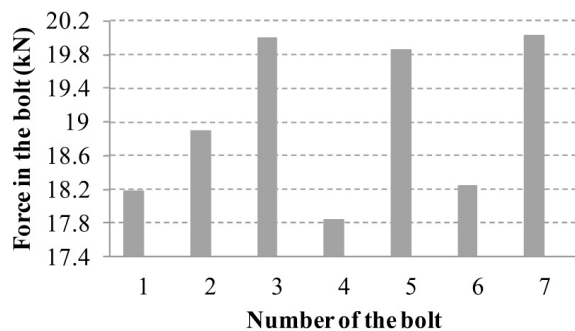
Fig. 5. Preload distribution in the bolts at the end of the tightening process of the multi-bolted system.

the joined elements during the tightening process and at the end of this process are highly variable and irregular.

The assessment of final values of the preload of the bolts and normal contact pressure can be executed using the following indicators expressed as a percentage:

$$W_1 = \frac{F_{fin,i} - F_{mi}}{F_{mi}} \cdot 100 \qquad (3)$$

$$W_2 = \frac{p_n - p_{n,a}}{p_{n,a}} \cdot 100 \qquad (4)$$

where: $F_{fin,i}$ denotes the final value of the preload of the *i*-th bolt at the end of the tightening process, F_{mi} is the initial value of the preload of the *i*-th bolt at the beginning of the tightening process, p_n is the value of normal contact pressure on the *n*-th contact surface, linked to the *n*-th node (Fig. 2b, $n = 1, 2, 3, …, 19$), and $p_{n,a}$ denotes the average value of normal contact pressure on the line joining the nodes shown in Figure 2b.

According to the introduced multi-bolted system model, the preload values of bolts may vary between -10.8 and 0.2%, relative to their initial values. At the same time, the values of normal contact pressure between the joined elements may vary in the range of -16.6 to 33.7%, in relation to their average values. The resulting calculation procedures can be used to optimise the preload of the individual bolts in order to ensure uniform pressure distribution at the interface between elements connected in the multi-bolted system. This can be accomplished by examining the impact of the tightening sequence of bolts on distribution of the preloads and normal contact pressure between the joined elements.

CONCLUSIONS

The described model of the multi-bolted system can be successfully used in the analysis of preload variations and normal contact pressure between joined elements variations in the case of any connection of flexible elements. The model can also provide the analysis on how does the tightening sequence affect the preload values in bolts before the preloaded connection is loaded by an external force.

REFERENCES

1. Abid M., Awan A.W. and Nash D.H. Determination of load capacity of a non-gasketed flange joint under combined internal pressure, axial and bending loading for safe strength and sealing. Journal of the Brazilian Society of Mechanical Sciences and Engineering, 36(3), 2014, 477–490.

2. Abid M., Khan A., Nash D.H., Hussain M. and Wajid H.A. Simulation of optimized bolt tightening strategies for gasketed flanged pipe joints. Procedia Engineering, 130, 2015, 204–213.

3. Ascione F. A preliminary numerical and experimental investigation on the shear stress distribution on multi-row bolted FRP joints. Mechanics Research Communications, 37(2), 2010, 164–168.

4. Brunesi E., Nascimbene R. and Rassati G.A. Seismic response of MRFs with partially restrained bolted beam-to-column connections through FE analyses. Journal of Constructional Steel Research, 107, 2015, 37–49.

5. Caliskan M. Evaluation of bonded and bolted repair techniques with finite element. Materials & Design, 27(10), 2006, 811–820.

6. Chen X. and Shi G. Finite element analysis and moment resistance of ultra-large capacity end-plate joints. Journal of Constructional Steel Research, 126, 2016, 153–162.

7. Cho S.-S., Shin C.S., Lee C.S., Chang H. and Lee K.W. Assessment of an engine cylinder head-block joint using finite element analysis. International Journal of Automotive Technology, 11(1), 2010, 75–80.

8. Chowdhury N.M., Chiu W.K., Wang J. and Chang P. Experimental and finite element studies of bolted, bonded and hybrid step lap joints of thick carbon fibre/epoxy panels used in aircraft structures. Composites Part B: Engineering, 100, 2016, 68–77.

9. Dacko M. and Nowak J. Analysis of blast loaded energy absorbing elements using LS-DYNA and MSC.DYTRAN systems (in Polish). Acta Mechanica et Automatica, 2(1), 2008, 13–20.

10. Esmaeili F., Zehsaz M., Chakherlou T.N. and Hasanifard S. Experimental and numerical study of the fatigue strength of double lap bolted joints and the effect of torque tightening on the fatigue life of jointed plates. Transactions of the Indian Institute of Metals, 67(4), 2014, 581–588.

11. Gray P.J. and McCarthy C.T. A global bolted joint model for finite element analysis of load distributions in multi-bolt composite joints. Composites Part B: Engineering, 41(4), 2010, 317–325.

12. Grzejda R. Designation of a normal stiffness characteristic for a contact joint between elements fastened in a multi-bolted connection. Diagnostyka, 15(2), 2014, 61–64.

13. Grzejda R. New method of modelling nonlinear multi-bolted systems. In M. Kleiber, T. Burczyński, K. Wilde, J. Górski, K. Winkelmann, and Ł. Smakosz (Eds.), Advances in Mechanics: Theoretical, Computational and Interdisciplinary Issues. Leiden: CRC Press, 2016, 213–216.

14. Grzejda R. Modelling nonlinear multi-bolted systems on the assembly state. Procedia Engineering, 206, 2017, 1808–1812.

15. Jakubowski A. and Schmidt H. Numerical investigations on the fatigue-relevant bolt stresses in preloaded ring flange connections with imperfections (in German). Stahlbau, 73(7), 2004, 517–524.

16. Karagiannis V., Málaga-Chuquitaype C. and Elghazouli A.Y. Behaviour of hybrid timber beam-to-tubular steel column moment connections. Engineering Structures, 131, 2017, 243–263.

17. Kędra R. and Rucka M. Diagnostics of bolted lap joint using guided wave propagation. Diagnostyka, 15(4), 2014, 35–40.

18. Kim J., Yoon J.-C. and Kang B.-S. Finite element analysis and modeling of structure with bolted joints. Applied Mathematical Modelling, 31(5), 2007, 895–911.

19. Li Z., Soga K., Wang F., Wright P. and Tsuno K. Behaviour of cast-iron tunnel segmental joint from the 3D FE analyses and development of a new bolt-spring model. Tunnelling and Underground Space Technology, 41, 2014, 176–192.

20. Liu X.C., He X.N., Wang H.X., Yang Z.W., Pu S.H. and Ailin Z. Bending-shear performance of column-to-column bolted flange connections in prefabricated multi-high-rise steel structures. Journal of Constructional Steel Research, 145, 2018, 28–48.

21. Luan Y., Guan Z.-Q., Cheng G.-D. and Liu S. A simplified nonlinear dynamic model for the analysis of pipe structures with bolted flange joints. Journal of Sound and Vibration, 331(2), 2012, 325–344.

22. Lupinetti K., Giannini F., Monti M. and Pernot J.-P. Multi-criteria retrieval of CAD assembly models. Journal of Computational Design and Engineering, 5(1), 2018, 41–53.

23. Moradi S. and Alam M.S. Multi-criteria optimization of lateral load-drift response of posttensioned steel beam-column connections. Engineering Structures, 130, 2017, 180–197.

24. Mourya R.K., Banerjee A. and Sreedhar B.K. Effect of creep on the failure probability of bolted flange joints. Engineering Failure Analysis, 50, 2015, 71–87.

25. Palenica P., Powałka B. and Grzejda R. Assessment of modal parameters of a building structure model. Springer Proceedings in Mathematics & Statistics, 181, 2016, 319–325.

26. Prinz G.S., Nussbaumer A., Borges L. and Khadka S. Experimental testing and simulation of bolted beam-column connections having thick extended endplates and multiple bolts per row. Engineering Structures, 59, 2014, 434–447.

27. Qiu M., Yan J., Zhao B., Chen L. and Bai Y. A finite-element analysis of the connecting bolts of slewing bearings based on the orthogonal method. Journal of Mechanical Science and Technology, 26(3), 2012, 883–887.

28. Reid J.D. and Hiser N.R. Detailed modeling of bolted joints with slippage. Finite Elements in Analysis and Design, 41(6), 2005, 547–562.

29. Sadigh M.A.S. and Marami G. Bearing and cleavage failure simulation of single lap bolted joint using finite element method. Transactions of the Indian Institute of Metals, 69(8), 2016, 1613–1622.

30. Smolnicki T. Derlukiewicz D. and Stańco M. Evaluation of load distribution in the superstructure rotation joint of single-bucket caterpillar excavators. Automation in Construction, 17(3), 2008, 218–223.

31. Zając K. and Krasoń W. Numerical models for the double suspension spring testing stand (in Polish). Mechanik, 88(5–6), 2015, 434–435.

32. Zhang L.Z., Liu Y., Sun J.C., Ma K., Cai R.L. and Guan K.S. Research on the assembly pattern of MMC bolted flange joint. Procedia Engineering, 130, 2015, 193–203.

33. Zhao Y., Yang C., Cai L., Shi W. and Liu Z. Surface contact stress-based nonlinear virtual material method for dynamic analysis of bolted joint of machine tool. Precision Engineering, 43, 2016, 230–240.